

High p_T Higgs signal for the LHC

V.A. Khoze^a, A.D. Martin^a and M.G. Ryskin^{a,b}

^a Department of Physics and Institute for Particle Physics Phenomenology, University of Durham, Durham, DH1 3LE

^b Petersburg Nuclear Physics Institute, Gatchina, St. Petersburg, 188300, Russia

Abstract

We show that the broad transverse momentum distribution of the Higgs boson produced by WW fusion can provide a viable way to identify $H \rightarrow b\bar{b}$ decays at the LHC, if particular kinematical configurations with large rapidity gaps are selected. We estimate the event rate of the signal and of the QCD $b\bar{b}$ background. We also discuss Higgs boson detection via the $H \rightarrow \tau\tau$ and $H \rightarrow WW^*$ decay modes.

1 Introduction

One of the main problems of searching for an intermediate mass Higgs boson at a hadronic collider is that it is hard to observe the dominant $H \rightarrow b\bar{b}$ decay mode due to the huge QCD $b\bar{b}$ background. An attractive possibility is to search for the process in which the Higgs boson is produced with a large rapidity gap on either side. The cleanest situation is double-diffractive exclusive production

$$pp \rightarrow p + H + p, \quad (1)$$

where the plus sign is used to indicate a rapidity gap (and similarly for $p\bar{p}$ collisions). However the predicted cross section is rather small [1, 2]¹. First, due to the proton form factors, the available phase space is strongly limited in the transverse momentum of the produced Higgs, $q_T \sim 1/R_p$ where R_p is the radius of the proton. Second, we must include the probability that the rapidity gaps survive the soft rescattering effects of spectator partons which may populate the gaps with secondary particles see, for instance, Ref. [7]. Third, the cross section is also suppressed by QCD radiative effects. That is by Sudakov-like suppression factors which allow for the possibility not to bremsstrahlung gluons which again may populate the rapidity gaps.

To enlarge the cross section we can consider semi-inclusive configurations [4] in which the protons may dissociate,

$$pp \rightarrow X + H + Y, \quad (2)$$

but where the Higgs is still isolated by rapidity gaps. In this case there is no proton-form-factor suppression and the Higgs bosons populate a much larger q_T phase space. Simultaneously the QCD radiative suppression becomes weaker, since the Sudakov double log takes the form $\sim \alpha_S \ln^2(M_H/\langle q_T \rangle)$, where now $\langle q_T \rangle \gg 1/R_p$. Moreover a significant contribution to process (2) comes from Higgs production via WW fusion (see Fig. 1(a)), where on account of the large W boson mass the cross section is rather flat in q_T . Furthermore, since this process is mediated by t -channel W exchange, which is a point-like colourless object, there is no corresponding bremsstrahlung in the central region [8] and thus the Sudakov suppression of the rapidity gaps does not occur.

Another contribution to (2) comes from the QCD subprocess $gg \rightarrow H$, where the colour flow of the hard t -channel gluons is screened by an accompanying, relatively soft, t -channel gluon as in Fig. 1(b). The double-gluon-exchange mechanism was first discussed in Ref. [3] (see also, for example, [9]) in terms of Higgs production by Pomeron-Pomeron fusion, using a non-perturbative two-gluon model of the Pomeron. However it was shown [1] that, at best, the $\mathbb{P}\mathbb{P} \rightarrow H$ mechanism gives a contribution comparable to $WW \rightarrow H$, for large rapidity gaps. On the other hand, \mathbb{P} fusion is the dominant mechanism for the QCD $b\bar{b}$ background to the semi-inclusive $H \rightarrow b\bar{b}$ production process (2). In this respect the exclusive process (1) appears to offer a better signal/background ratio since $\mathbb{P}\mathbb{P} \rightarrow q\bar{q}$ vanishes as $m_q/E_T \rightarrow 0$ in the forward direction due to a specific $J_z = 0$ selection rule [10, 11, 2], and $q\bar{q}g$ production

¹Note that the existing literature shows a wide range of predictions for this cross section which vary by many orders of magnitude. These can be found, for example, in [3, 4, 5, 6]. It is worthwhile to mention that the recent estimates of Refs. [1, 2] give the lowest cross section among those listed in [6].

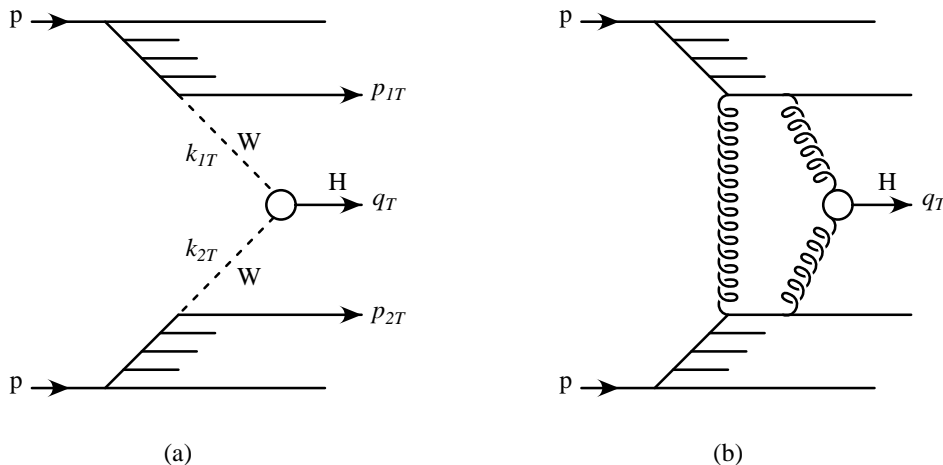


Figure 1: Semi-inclusive Higgs production, $pp \rightarrow X + H + Y$, via (a) WW fusion and (b) Pomeron-Pomeron fusion, where the QCD Pomeron is described by two-gluon exchange.

is suppressed. E_T is the transverse energy of one of the jets. As mentioned above, the only problem is that the predicted cross section is too small to exploit the exclusive Higgs signal, at least at the Tevatron.

For semi-inclusive production there is no $J_z = 0$ selection rule to suppress the $b\bar{b}$ background. Moreover the expected $b\bar{b}$ mass resolution is worse than in the exclusive case. Thus the signal-to-background ratio is relatively small [12],

$$\frac{S}{B} \sim 0.01 \left(\frac{M_H}{100 \text{ GeV}} \right)^3 \left(\frac{4 \text{ GeV}}{\Delta M} \right), \quad (3)$$

where ΔM is the mass resolution. Nevertheless, we will show that it is possible to select a kinematic domain where semi-inclusive Higgs production may be identified at the LHC. We exploit the much flatter q_T dependence of semi-inclusive production and select Higgs candidates with large q_T , say $q_T > q_0$. We show that it is possible to tune the q_T and the rapidity cuts to select a domain where the predicted cross section is not too small so that the Higgs stands out from the background². We use the formalism of Ref. [1], and include the recent evaluations of the survival probabilities of the rapidity gaps [14, 15]. The calculation of the $H \rightarrow b\bar{b}$ signal is described in Section 2, and the computation of the QCD $b\bar{b}$ background is the subject of Section 3. Numerical predictions for the signal and background are given in Section 4 for particular choices of the large $q_T > q_0$ cut and of the rapidity gaps.

In Section 5 we discuss the possibility of observing the Higgs boson via process (2) in the $H \rightarrow \tau^+\tau^-$ decay mode or, as the Higgs becomes heavier, by $H \rightarrow WW^*$ decays. In both of these cases the branching ratio for an intermediate mass Higgs is much smaller than that for $H \rightarrow b\bar{b}$, but there is almost no QCD background, provided that we select events with rapidity gaps. In Section 6 we give our conclusions.

²The idea to increase the signal-to-background ratio by selecting high q_T Higgs inclusively produced by WW fusion, and to suppress the $q\bar{q} \rightarrow ZZ$ background which is steeper in q_T , was originally proposed in [13].

2 The $WW \rightarrow H \rightarrow b\bar{b}$ signal at large q_T

The cross section for electroweak Higgs production of Fig. 1(a) is well known [16, 17]. To obtain the q_T distribution of the Higgs we need to perform the integration [13]

$$\int \frac{d^2 k_{1T} d^2 k_{2T}}{(k_{1T}^2 + M_W^2)(k_{2T}^2 + M_W^2)} \delta^{(2)}(\mathbf{k}_{1T} + \mathbf{k}_{2T} - \mathbf{q}_T) \dots, \quad (4)$$

where $\mathbf{k}_{1T,2T}$ are the transverse momenta of the exchanged W^\pm bosons. The parton-parton luminosity, which controls the normalisation of the cross section, was calculated using MRST partons [18]. At first sight it appears sufficient to evaluate the parton distributions at scales k_{iT}^2 , and at the corresponding x values, but the situation is not so trivial. The problem is that the partons coupled to the W bosons are emitted with rather large transverse momenta, p_{1T} and p_{2T} , and materialise as jets with secondaries which may lie inside the rapidity gaps. In order not to have jets with rapidity close to that of the Higgs boson, that is to have $|\eta_{\text{jet}}| > |\eta_{\text{min}}|$, we have to sample partons with light cone momentum fractions $x_i > x_{\text{min}}^i$, with

$$x_{\text{min}}^i = (M_H + p_{iT} \exp(|\eta_{\text{min}}^i|)/\sqrt{s}, \quad (5)$$

see also [11]. Here we have assumed that the Higgs boson is produced with rapidity³ $\eta_H = 0$.

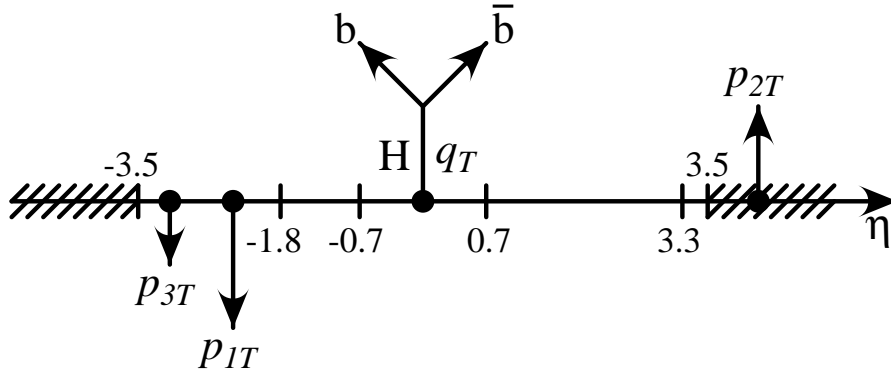


Figure 2: The particular configuration of the rapidity gaps of the process of Fig. 1(a) used to calculate the cross sections given in Table 1. We also include the configuration in which the diagram is reflected in the origin. We show the configuration for $\eta_H = 0$, but we allow $\eta_H \neq 0$ and apply an overall Lorentz boost accordingly.

In order to retain a large part of the cross section, and also to have a favourable signal-to-background ratio, the experimental cuts must be chosen with care. For illustration we calculate the event rates for the particular configuration shown in Fig. 2. We require that the jet, say jet 2, with the smaller p_T ($p_{2T} < p_{1T}$) satisfies

$$\Delta\eta_2 = \eta_2 - \eta_H > 3.3, \quad (6)$$

³For $\eta_H \neq 0$, we simply make a boost and multiply the right-hand- side of (5) by $\exp(\eta_H)$.

while we allow jet 1 with the largest p_T to be possibly closer to the Higgs

$$\Delta\eta_1 = \eta_H - \eta_1 > 1.8. \quad (7)$$

Thus we have a rapidity gap $\Delta\eta > 5.1$, except for the $H \rightarrow b\bar{b}$ decay. Moreover, within the overall rapidity interval $|\eta| < 3.5$ we require no other jets, apart from the b, \bar{b} jets and possibly the two jets coupled to the exchanged bosons. However we allow for the possibility of one extra jet arising from the usual parton structure function evolution associated with the larger p_T jet lying in the interval with the smaller $|\eta_{\min}|$, see Fig. 2. In the leading log approximation the separation between these two jets (denoted p_{1T} and p_{3T} on Fig. 2) should be $\Delta\eta \gg 1$, but in reality the expectation is $\Delta\eta \sim 2$. We emphasize that the p_{iT} jets do not have to be within the rapidity interval $|\eta| < 3.5$. The requirement is that the p_{1T} and p_{3T} jets have $\eta < -1.8$, and the p_{2T} jet has $\eta > 3.3$. The configuration reflected in the origin ($\eta = 0$) is also allowed. This combination of rapidity gaps and jets (together with the possible tagging of b -jets and the reconstruction of their vertices) can provide a strong signature for Higgs production. The predicted cross sections corresponding to the configurations allowed by Fig. 2 are presented in Section 4.

3 The QCD $b\bar{b}$ background

The $b\bar{b}$ background is calculated using the formalism described in Ref. [11] for the same jet configurations as given above. The cross section is given by the convolution of the parton-parton luminosity and the production of $b\bar{b}$ in a colour-singlet configuration via the fusion of two BFKL Pomerons, see Fig. 3. The $IP \rightarrow b\bar{b}$ part of the cross section is given by

$$\frac{d\sigma}{dE_T^2 d\eta_{b\bar{b}} d\Delta\eta} = \alpha_S^4 \frac{81}{64\pi^2} \mathcal{I} \left[\frac{\pi\alpha_S^2(E_T^2)}{6E_T^2 M_{b\bar{b}}^2} \left(1 - \frac{2E_T^2}{M_{b\bar{b}}^2} \right) \right], \quad (8)$$

where $\Delta\eta = |\eta_b - \eta_{\bar{b}}|$ and the expression in brackets is the $gg \rightarrow b\bar{b}$ colour-singlet hard subprocess cross section $d\hat{\sigma}/d\hat{t}$ [10, 11]. The QCD Pomerons, each represented by two-gluon exchange, are described by BFKL non-forward amplitudes [11, 19]. Non-forward because the dominant contribution comes from the asymmetric region where the transverse momentum Q_T carried by the screening gluon is much smaller than the total momentum transfer carried by the Pomeron. Due to the asymmetry we have, besides $\Delta\eta_i$, a second logarithm, $\ln(k_{iT}^2/Q_T^2)$ in the BFKL evolution. The summation of the double logarithms accounts for the probability not to emit extra gluons within the rapidity gap covered by the Pomeron. In addition, we must include the usual Sudakov form factors which arise from the requirement that there is no gluon emission in the intervals k_{iT} to E_T . The factor \mathcal{I} in the cross section formula (8) arises from the integration over the t -channel gluon loop in the amplitude of the process shown in Fig. 3. \mathcal{I} contains the BFKL amplitude and all the suppression factors arising from the requirement that there should be no gluon emission in the rapidity gaps, and it is given by eq. (27) of Ref. [11].

Of course the $gg \rightarrow b\bar{b}$ cross section, $d\hat{\sigma}/d\hat{t}$, becomes too large at small E_T , see (8). Thus, in order to suppress this QCD $b\bar{b}$ background we impose a cut $E_T > 50$ GeV in the $b\bar{b}$ rest

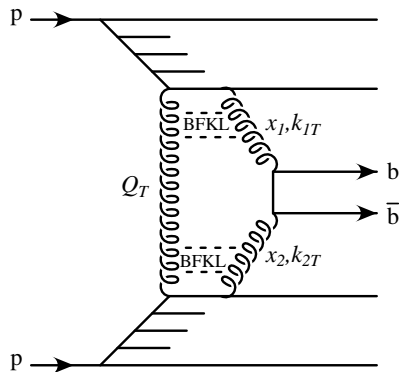


Figure 3: The QCD $b\bar{b}$ background process to the $H \rightarrow b\bar{b}$ signal of Fig. 1(a).

frame. For a dijet system of mass $M_{b\bar{b}} = 115$ GeV this corresponds to the restriction that b and \bar{b} jets have polar angles $\theta > 60^\circ$. The same cuts must be applied to the $H \rightarrow b\bar{b}$ decay and as a consequence we lose about half of the signal. In terms of rapidities it means that we select events with jets with $\Delta\eta = |\eta_b - \eta_{\bar{b}}| < 1.4$, see Fig. 2.

4 Predicted rates for $H \rightarrow b\bar{b}$ and background

We have integrated the cross sections described above over the $b\bar{b}$ transverse momentum interval $q_T > q_0$ (with $q_0 = 25$ or 40 GeV), and over the rapidity of the $b\bar{b}$ pair. The main contribution comes from the central region, $|\eta_{b\bar{b}}| < 1.5$. We use a fixed⁴ coupling $\alpha_S = 0.17$, which represents the typical coupling in the selected kinematical domain, see also Ref. [20].

In Table 1 we present the signal and background rates for two different values of the Higgs boson mass and for the two choices of the $b\bar{b}$ q_T cut. The upper and lower halves of the Table correspond to different treatments of the survival probabilities of the rapidity gaps, as explained below. The column of values of σ_H shows the $WW \rightarrow H$ cross sections which allow for the rapidity gaps of Fig. 2 and for the $q_T > q_0$ cut, but which do *not* include the $H \rightarrow b\bar{b}$ branching ratio, or the $\theta > 60^\circ$ jet cut or for the efficiency of the b and \bar{b} jet tagging. If we include these latter effects⁵ then we have the ‘useful’ $WW \rightarrow H \rightarrow b\bar{b}$ signal shown in the next column in Table 1, followed by the cross section for the QCD $pp \rightarrow b\bar{b}$ background.

These cross section values shown in the Table correspond to (8) convoluted with the parton-parton luminosity, with (8) integrated over the b and \bar{b} jet rapidities, $\eta_{b\bar{b}}$ and $\Delta\eta$, and over a small bin of transverse energy which corresponds to $b\bar{b}$ events in the Higgs mass interval.

⁴In fact, using running α_S in the double logarithmic form of the BFKL non-forward amplitude one obtains, after the loop integration over Q_T , essentially the same result ($\sim \alpha_S(k_{iT}^2)/\Delta\eta$) as for the case of fixed α_S . Since we select $b\bar{b}$ events with $q_T > 25$ GeV, the transverse momentum of the harder gluon is in the region 10-30 GeV, corresponding to $\alpha_S = 0.17$.

⁵We assume a combined efficiency of 0.7 for identifying both b and \bar{b} jets.

M_H	$q_T >$	Total σ_H	Signal $\sigma_{H \rightarrow b\bar{b}}$	Background $\sigma_{IP \rightarrow b\bar{b}}$	$\sigma_{H \rightarrow \tau\tau}$	$\sigma_{H \rightarrow WW^*}$
115	25	38	9.6	142	0.27 (0.54)	3.1
	40	21	5.3	38	0.15	1.7
140	25	29	3.3	61	0.09 (0.19)	16
	40	14	1.6	20	0.04	7.6
115	25	61	16	116	0.44 (0.82)	5.0
	40	35	9	36	0.25	2.8
140	25	48	5.4	51	0.15 (0.29)	27
	40	24	2.7	19	0.08	13

Table 1: M_H and q_T are in GeV. The cross sections are in fb, and correspond to the rapidity cuts shown in Fig. 2, *except* for the $H \rightarrow \tau\tau$ values shown in brackets which correspond to the softer cuts given in the text. Unlike the total σ_H , the $H \rightarrow b\bar{b}$ signal and background cross sections include the $H \rightarrow b\bar{b}$ branching fraction, the b and \bar{b} tagging efficiency and the polar angle $\theta > 60^\circ$ cut on the b and \bar{b} jets. The upper and lower halves of the Table correspond to using the survival probabilities of the rapidity gaps that were determined in Refs. [14] and [15] respectively.

The smallness of this interval is limited by the experimental jet resolution. Here we assume $\Delta E_T = 4$ GeV in the $b\bar{b}$ centre-of-mass frame.

The predictions in the top half of the Table correspond to using the values of the survival probability S^2 listed in the double-diffractive (DD) column of Table 1 of Ref. [14] for $\sqrt{s} = 14$ TeV. That is $S^2 = 0.15$ for the $WW \rightarrow H$ signal (where we assume that the spatial distribution of the quarks is described by the electromagnetic form factor of the proton with slope 5.5 GeV^{-2}) and $S^2 = 0.10$ for the $IP \rightarrow b\bar{b}$ background (where the slope of the corresponding distribution is taken to be 4 GeV^{-2}). In this case for an integrated luminosity of 100 fb^{-1} at the LHC⁶ we have, for $M_H = 115$ GeV and $q_T > 25$ GeV, about 1000 $WW \rightarrow H \rightarrow b\bar{b}$ identified events sitting on top of a QCD $b\bar{b}$ background of 14,000 events, see Table 1. This would give an 8 standard-deviation signal. Increasing the q_T cut improves the signal/background ratio, but decreases the number of events, so in fact the quality of the signal declines if, for example, we were to choose the cut $q_T > q_0$ with $q_0 = 50$ GeV.

The above values of the survival probability S^2 of the rapidity gaps were calculated [14] using a two-channel rescattering eikonal in which the diffractive eigen-channels have different cross sections of absorption, $\sigma_0(1 \pm \gamma)$ with $\gamma = 0.4$. In Ref. [15], arguments were given that the lower cross section arises mainly from the valence quark configurations and that the higher cross section comes dominantly from the gluon and sea quark configurations. Adopting this

⁶Of course, at large LHC luminosities secondary particles produced in ‘pile-up’ events may fill the rapidity gaps. However we hope that it is possible to select experimentally tracks coming from the same vertex and so separate the particles which belong to the event of interest, in which a Higgs boson is produced with a large rapidity gap on either side.

simplified model would give a larger S^2 for $WW \rightarrow H$ production⁷ where the valence quarks play a dominant role, and a lower S^2 for the QCD $\mathbb{P}\mathbb{P} \rightarrow b\bar{b}$ background, which originates from the gluons. Of course, now the ‘survival’ factor S^2 depends on the values of the mass and q_T of the Higgs boson (or $b\bar{b}$ -pair). For smaller values of the mass and q_T the screening corrections are stronger, since there is a larger contribution caused by gluon-gluon collisions. For a pure gluon-gluon interaction the factor $S_{gg}^2 = 0.033$ in this model, while for a valence quark collision $S_{qq}^2 = 0.37$ (and $S_{qg}^2 = 0.15$ for the case of gluon and valence quark collisions).

Averaging over all contributions we obtain a suppression factor $S^2 \simeq 0.08 - 0.1$ for QCD $b\bar{b}$ -pair production, whereas $S^2 \simeq 0.24 - 0.26$ for Higgs production via the WW -fusion. The limits of the range of S^2 correspond respectively to the largest and smallest values of q_T and mass in Table 1. As was expected the factor S^2 is closer to S_{gg}^2 for the case of QCD $b\bar{b}$ double-Pomeron production, but for Higgs production it is closer to the S_{qq}^2 value. The results for this model are shown in the lower half of Table 1. Thus for a luminosity 100 fb^{-1} , $M_H = 115 \text{ GeV}$ and $q_T > 25 \text{ GeV}$, we have a chance to identify 1600 $H \rightarrow b\bar{b}$ events sitting on a background of 11,600 events. This would be about a 15 standard-deviation effect. To put it another way, a luminosity of 12 fb^{-1} would be enough to achieve a 5 standard-deviation signal.

Of course, the above cuts and corresponding predictions are just examples. The experimental cuts should be optimized, taking into account the specifics of the detectors. Also note that there is a factor of two uncertainty in the background prediction due to the use of the double log approximation. Fortunately the single log contributions are suppressed in our asymmetric two-gluon-exchange domain, so that we are not so sensitive to the uncertain higher-order BFKL effects.

5 $WW \rightarrow H \rightarrow \tau^+\tau^-$, WW^* and ZZ^* high q_T Higgs signals

Another possibility is to observe the $H \rightarrow \tau^+\tau^-$ decay mode, where there is practically no QCD background. Of course, the small $H \rightarrow \tau^+\tau^-$ branching fraction leads to a small cross section, as shown in Table 1. However we may increase the signal by choosing softer cuts. For example, the values of the cross section shown in brackets correspond to the cut $q_T > 20 \text{ GeV}$, and the rapidity cuts of the accompanying jets $|\eta_1| > 1.5$ and $|\eta_2| > 2.9$ (for the case $\eta_H = 0$, as in Fig. 2).

The main background for the $H \rightarrow \tau^+\tau^-$ signal comes from the central production of the Z boson and its subsequent $\tau^+\tau^-$ decay. If we were able to reconstruct the mass of the $\tau^+\tau^-$ pair it would be easy to identify $H \rightarrow \tau^+\tau^-$ events. Unfortunately there are two unobserved ν_τ neutrinos from the τ decays. It does not mean $M_{\tau\tau}$ is completely unknown. It may be estimated from the decay configurations⁸, but the accuracy is not so good. The cross section

⁷In principle we can measure the survival probability S^2 for the gaps surrounding $WW \rightarrow H$ fusion by observing the closely related central production of a Z boson with the same rapidity gap and jet signature [21].

⁸For example, in the Higgs rest frame the τ^+ and τ^- emerge back-to-back. Since $M_H \gg m_\tau$, the direction of the decay products is, to a good approximation, collinear with the parent τ . Hence we can find the Lorentz boost, $\gamma = \mathbf{q}_H/M_H$, needed to restore the collinearity of the two τ 's. Also the transverse momentum \mathbf{q}_T can be measured as the momentum balancing that of the jets or simply as the missing E_T . Hence we can estimate the value of M_H .

for the central production of a Z boson, accompanied by two jets, has been calculated for the LHC energy in Ref. [22], however without including the survival probability S^2 of the rapidity gaps. If we include S^2 in their results then the $(Z \rightarrow \tau\tau) + 2$ jet cross section is predicted to be about 6 fb for the cuts similar to the ones that were chosen for the larger $H \rightarrow \tau^+\tau^-$ signal shown in brackets in Table 1. The background is therefore an order of magnitude, or more, larger than the Higgs signal. Nevertheless, if the mass resolution is not too bad, there is a chance to identify the $H \rightarrow \tau^+\tau^-$ signal. Clearly the $Z \rightarrow \tau^+\tau^-$ decay mode will pose less of a problem the higher the value of M_H .

For larger values of M_H the $H \rightarrow \tau^+\tau^-$ decay mode decreases as the $H \rightarrow WW^*$ decay opens up. Therefore for the heavier Higgs boson it is more promising to search for the $H \rightarrow WW^*$ and $H \rightarrow ZZ^*$ signals⁹. The corresponding cross sections are listed in the last column of Table 1. We see, for $M_H = 140$ GeV, that the $H \rightarrow WW^*$ cross section is about 20 fb. Again there is practically no QCD background in the configuration with two large rapidity gaps either side of the parent Higgs. Of course, we must allow for the detection efficiency of the various decay modes. It is difficult to extract the value of M_H from the leptonic decays of both the W and W^* . However it may be possible to use the decay configuration $W \rightarrow$ two quark jets and $W^* \rightarrow \ell\nu$. On the other hand, the $H \rightarrow ZZ^* \rightarrow 4$ leptons process will provide a rather clean signature.

Finally, we emphasize if $M_H > 2 M_Z$, then adding the rapidity signature to the gold-plated $H \rightarrow ZZ \rightarrow 4$ lepton channel, would practically eliminate the background due to $q\bar{q} \rightarrow ZZ$. The Higgs signal may be thus purified at the expense of introducing the survival probability factor S^2 , and in this way allow a more precise study of the properties of the Higgs boson.

Acknowledgements

One of us (VAK) thanks the Leverhulme Trust for a Fellowship. This work was partially supported by the UK Particle Physics and Astronomy Research Council, by the EU Framework TMR programme, contract FMRX-CT98-0194 (DG 12-MIHT) and by the RFFI grants 00-15-96610 and 01-02-17095.

⁹It was shown in Ref. [23] that the $H \rightarrow WW^* \rightarrow \ell^+\ell^- +$ missing p_T signal may be considered as a discovery mode, even for a light ($M_H = 115$ GeV) Higgs boson, if one selects events where the Higgs is produced by WW fusion in association with two light quark jets. The corresponding kinematics (similar to that shown in Fig. 2) were discussed in detail in [23]. However another criteria for the large rapidity gap was used in [23] (within the gap no jets with $p_T > 20$ GeV are permitted) and so another gap-survival factor was used.

References

- [1] V.A. Khoze, A.D. Martin and M.G. Ryskin, Eur. Phys. J. **C14** (2000) 525.
- [2] V.A. Khoze, A.D. Martin and M.G. Ryskin, hep-ph/0011393, Eur. Phys. J. **C** (in press).
- [3] A. Bialas and P.V. Landshoff, Phys. Lett. **B256** (1991) 540.
- [4] V.A. Khoze, A.D. Martin and M.G. Ryskin, Phys. Lett. **B401** (1997) 330 and references therein.
- [5] D. Kharzeev and E.M. Levin, Phys. Rev. **D63** (2001) 073004 and references therein.
- [6] M.G. Albrow and A. Rostovtsev, hep-ph/0009336 and references therein.
- [7] B.J. Bjorken, Int. J. Mod. Phys. **A7** (1992) 4189.
- [8] Yu.L. Dokshitzer, V.A. Khoze and S.I. Troyan, Sov. J. Nucl. Phys. **46** (1987) 712;
Yu.L. Dokshitzer, V.A. Khoze and T. Sjöstrand, Phys. Lett. **B274** (1992) 116.
- [9] J.R. Cuddeh and O.F. Hernandez, Nucl. Phys. **B471** (1996) 471;
E.M. Levin, hep-ph/9912403.
- [10] J. Pumplin, Phys. Rev. **D52** (1995) 1477.
- [11] A.D. Martin, M.G. Ryskin and V.A. Khoze, Phys. Rev. **D56** (1997) 5867.
- [12] V.A. Khoze, A.D. Martin and M.G. Ryskin, hep-ph/0103007.
- [13] R.N. Cahn, S.D. Ellis, R. Kleiss and W.J. Stirling, Phys. Rev. **D35** (1987) 1626.
- [14] V.A. Khoze, A.D. Martin and M.G. Ryskin, Eur. Phys. J. **C18** (2000) 167.
- [15] A.B. Kaidalov, V.A. Khoze, A.D. Martin and M.G. Ryskin, to be published.
- [16] J. Gunion, H. Haber, G. Kane and S. Dawson, “*The Higgs Hunter’s Guide*”, Addison-Wesley, Reading, Massachusetts, 1990).
- [17] M. Spira, Fortsch. Phys. **46** (1998) 203.
- [18] A.D. Martin, R.G. Roberts, W.J. Stirling and R.S. Thorne, Eur. Phys. J. **C14** (2000) 133.
- [19] J.R. Forshaw and M.G. Ryskin, Z. Phys. **C68** (1995) 137.
- [20] B. Cox, J.R. Forshaw and L. Lönnblad, hep-ph/9912489.
- [21] H. Chehime and D. Zeppenfeld, Phys. Rev. **D47** (1993) 3898.
- [22] D. Rainwater and D. Zeppenfeld, Phys. Rev. **D54** (1996) 6680.
- [23] N. Kauer, T. Plehn, D. Rainwater and D. Zeppenfeld, Phys. Lett. **B503** (2001) 113.